Droplet CFD

In Energent's Variable Phase Turbine [1-2] (VPT) the fluid at the inlet is liquid, flashes inside the nozzle upstream of the turbine rotor, and is two-phase inside the rotor blade passage. A previous article [3] discussed calculating the trajectories of droplets inside the turbine rotor.

In the converging section of the nozzle, the pressure decreases. When it declines to the saturation pressure, vapor bubbles form. At this pressure, the liquid is the continuous phase, the vapor the dispersed phase. With a continued decrease in pressure, eventually the liquid is the dispersed phase as droplets. The development of the dispersed phase, from the formation of vapor bubbles as the dispersed phase, the transition to liquid droplets being the dispersed phase, and the droplet breakup is not an easy task to model in computational fluid dynamics (CFD).

At first CFD is being used to investigate the flow field around droplets. An objective is to use the information gained from the calculations to develop a reduced order model that can be incorporated into traditional CFD codes and 1-D nozzle codes. Experimental work has been found for model problems to begin investigating computationally. By finding problems to study that have been investigated experimentally, the methodology used in the CFD simulations can be validated.

A starting point is to examine the flow field around a single liquid droplet. An objective is to study the breakup of the droplet. In the meantime, the breakup of a 2-D water column subjected to a shock wave is investigated, for which there is experimental data from Tohoku University [4], Japan. By considering first the breakup of a 2-D liquid column instead of a 3-D spherical droplet, the computational cost is reduced.

Initially the calculations were done by solving the Euler equations. Although the physical viscosity is ignored, numerical viscosity is still present. Figure 1 is a series of snapshots of a liquid column breaking up, displayed as a Schlieren image of the density gradient.

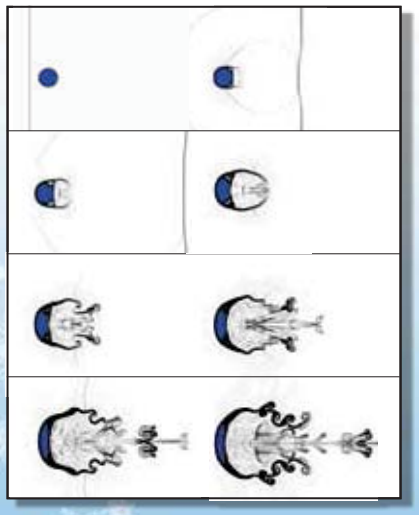

Figure 1 Schlieren images of a shock wave impinging on a liquid

The momentum interaction between the dispersed liquid phase and the continuous vapor phase is through the droplet drag, which is characterized by the drag coefficient. During the droplet breakup a question to answer is how to model the drag.

Drag coefficient

$$C_D = \frac{D}{\frac{1}{2}\rho u^2 S} = \frac{ma}{\frac{1}{2}\rho_G u_G - u^2 d}$$

S = frontal area of cylinder, in 2-D the diameter

The liquid cylinder's center of mass was obtained from the CFD results during the time interval while there is no mass flux through the boundaries. Its position, velocity and acceleration were calculated. Plotted in Figure 2 are drag coefficients for the incident planar shock with Mach numbers of 1.3, 1.5 and 1.7. The initial column diameter is used to non-dimensionalize the drag coefficient.

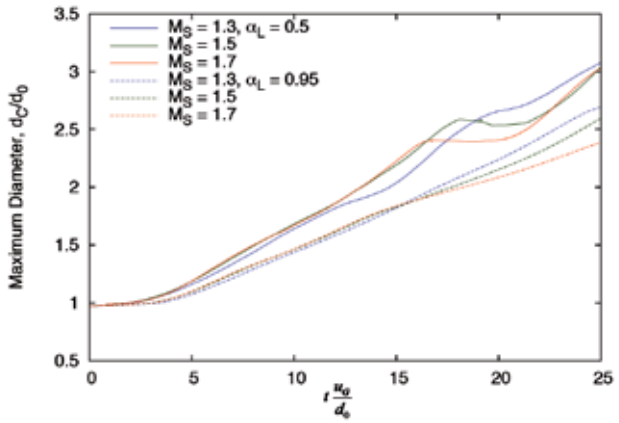

Figure 2 Drag coefficient non-dimensionalized using the initial column diameter, for several different incident Mach numbers.

From the calculation, the frontal diameter of the deforming cylinder was obtained as a function of time for different values of the liquid volume fraction threshold, Figure 3.

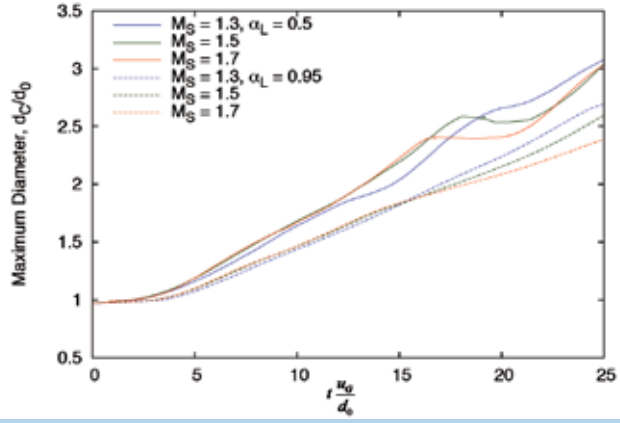

Figure 3 Frontal diameter of the deforming cylinder for two different threshold values of the liquid volume fraction, for several different incident Mach numbers.

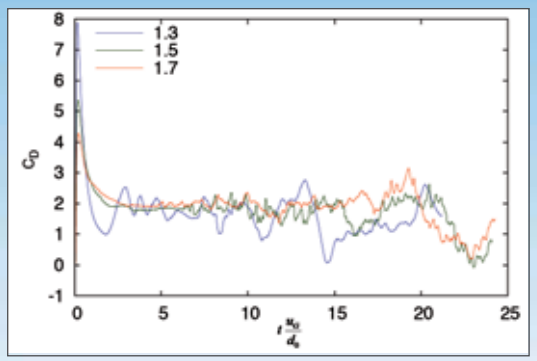

Figure 4 Drag coefficient non-dimensionalized using the deforming column frontal diameter, for a threshold value of 0.95 of the liquid volume fraction, for several different incident Mach numbers.

By using the actual column diameter instead of the initial diameter, the drag coefficient shows significantly less variation during the breakup period that is simulated, Figure 4.

In the application of interest, the droplet is not in isolation, but is part of a cloud. At Sandia National Laboratory [5], experiments have been conducted on a planar shock wave impacting a curtain of solid particles.

The simulation focuses on the early stage of the experiment when the particles have not yet moved and can be assumed to be fixed in space. The 3-D particle cloud is modeled by an array of staggered cylinders, Figure . With the stagger arrangement used, the open cross sectional area varies by less than 1.5%, Figure 6. The volume fraction is nearly constant through the curtain. For this 2-D model, the Euler equations are solved. The numerical method implicitly contains numerical viscosity.

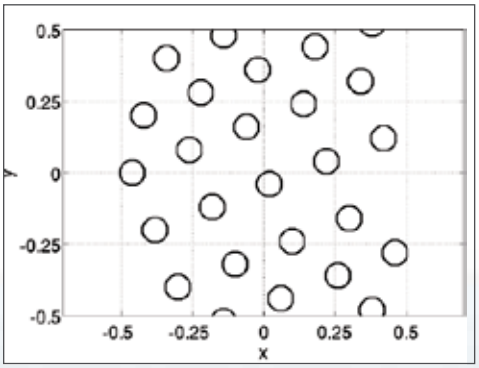

Figure 5 Array of staggered cylinders.

Figure 6 Open cross sectional area of the cylinder array.

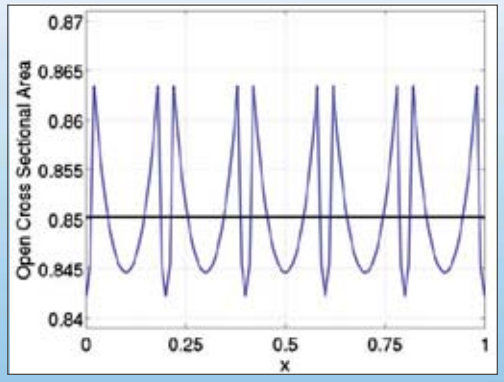

Figure 7 shows the reflected and transmitted shock waves, as well as the unsteady flow conditions both inside and behind the cylinder cloud.

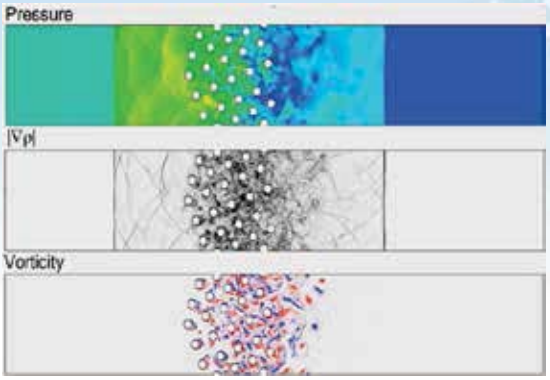

Figure 7 Flow variables of the 2-D calculation at t=3.5.

A one-dimensional model is derived from the volume-averaged Navier-Stokes equations, where the viscous stresses within the continuous phase are assumed to be negligible, but the momentum coupling terms are still considered. The 1-D model equations that were solved do not include the unclosed fluctuation terms created during the volume-averaging procedure, such as the Reynolds stress. This is a reasonable assumption in dilute multiphase flows. However, in dense flows this assumption may not be appropriate.

The miscellaneous particle forces are assumed to be included in the drag coefficient for the quasi-steady drag force on a single particle

$$F_i^{qs} = \frac{1}{2}\rho C_D A_p \mid u_i - v_i \mid (u_i - v_i)$$

where A_p is the particle cross-section, C_D is the drag coefficient, and u and v are the continuous and dispersed phase velocities, respectively. For the time period considered the particle is fixed in space, so $v_i = 0$. For the 2-D particle, the cross-section area is its diameter, D_p. The drag coefficient C_D was determined by finding the value that best matches the reflected and transmitted shock locations and magnitudes of the 2-D solution.

Figure 8 - Figure 10 compare the solution of the 1-D model with a planar average of the 2-D result at the non-dimensionalized time of 3.5. The particle curtain is located between -0.5 < x < 0.5. For the plots of density and velocity, the 2-D results appear to oscillate around the 1-D model results for a significant portion of the solution. For these profiles, two additional cases are shown where the drag coefficient is increased and decreased by 30%. Small, yet noticeable, differences can be observed in the shock locations. This suggests that the methodology used is adequate to evaluate an overall mean drag coefficient.

continued on page 8

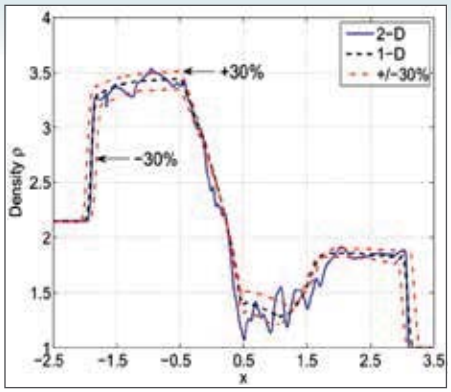

Figure 8 Comparison of the density from the 1-D model and with the planar average of the 2-D model at t=3.5. In addition for the 1-D model, the drag coefficient was varied by +/- 30%.

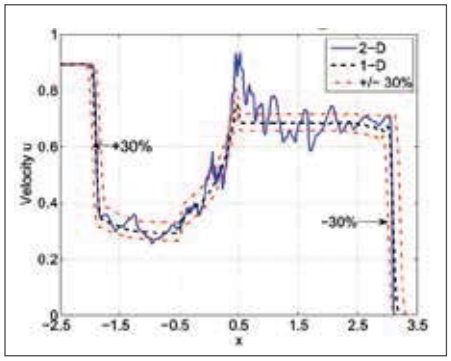

Figure 9 Comparison of the velocity from the 1-D model with the planar average of the 2-D model at t=3.5. In addition for the 1-D model, the drag coefficient was varied by +/- 30%.

In Figure 10 the planar averaged pressure in the 2-D result is consistently lower than that predicted by the 1-D model inside the particle cloud and downstream of the trailing edge until x 1.5. This is attributed to the fluctuations associated with the vortical structures (see Figure 7), which is a behavior that the 1-D model, in its current form, is incapable of reproducing. Also shown is the sum of the volume-averaged pressure $p_T = (p) + \alpha_c (\rho u'' u'')$

The effective total Reynolds pressure better matches the 1-D model solution inside the cloud and unsteady region. The 1-D model overestimates the static pressure by including the energy that should be contained in turbulent kinetic energy. This flow is too dense to neglect the Reynolds stress terms.

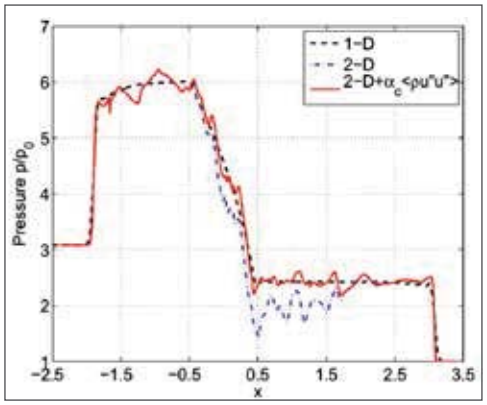

Figure 10 Comparison of the pressure from the 1-D model with the planar average of the 2-D model at t=3.5, and with the Reynolds stress term included.

By examining how 2-D and eventually 3-D computations compare with experimental data, we would have more confidence in the reduced order model that we want to develop to describe the 3-D phenomena of flow around droplets.

[1] Lance Hays, "The Energent Variable Phase Turbine expands liquids or supercritical fluids used in refrigeration," *FrostByte*, Summer 2008, pages 1, 4.

[2] Lance Hays, "Cryogenic Liquid Expanders," *FrostByte*, Summer 2011, page 2.

[3] Ron Franz, "Droplet Trajectories in a Turbine Rotor," *FrostByte*, Winter 2011, page 7.

[4] D. Igra and K. Takayama, "Experimental Investigation of Two Cylindrical Water Columns Subjected to Planar Shock Wave Loading," *Journal of Fluids Engineering*, 125: 325–331, 2003.

[5] Wagner, J. L., Beresh, S. J., Kearney, S. P., Trott, W. M., Castaneda, J. N., Pruett, B. O., Baer, M. R., "A multiphase shock tube for shock wave interactions with dense particle fields," *Experiments in Fluids* 52 (6), 1507–1517, Feb. 2012.

CRYOGENIC INDUSTRIES

25720 Jefferson Avenue
Murrieta, CA 92562-9524 USA

CRYOGENIC INDUSTRIES TO RELOCATE HEADQUARTERS

This Fall Cryogenic Industries will relocate its headquarters offices from Murrieta, CA to Temecula, CA. The new facilities will house administrative, finance, treasury, legal, internal audit, regulatory compliance, human resources and tax functions. An announcement with the new address and telephone numbers will be made at the time of the relocation.

North America

ACD • Atlanta • California • Houston • Pittsburgh • Red Deer • Toronto
Cosmodyne • Cryoquip • Energent

South America

ACD • Cryoquip

Australia

Cryoquip

South Africa

Cosmodyne • Durban

Europe

ACD Cryo • Cryoquip

Middle East

United Arab Emirates, Dubai

Asia

ACD • China • Korea • Malaysia • India
Cryoquip • China • Malaysia • India
Rhine Engineering • India